DEALING WITH MOTOR WINDING PROBLEMS CAUSED BY INVERTER DRIVES

By:
Mark Fenger, Steven R. Campbell, Iris Power Engineering Inc.
Jan Pedersen, Techwise A/S

Abstract: Random wound stator windings operating in utility and industrial plants have failed when exposed to the fast rise-time voltage surges coming from inverters. Studies show that the failure is due to a combination of bad luck in specific motor installations (resonance phenomena caused by power cable length and surge impedance ratios) together with the fact that modern inverted-fed drives (IFD's) create tens of thousands of surges per socond with rise-times as fast as 50ns. Measurements on motors show that these surges create partial discharges (also called corona) and these discharges may eventually destroy the turn-to-turn and/or phase-to-phase insulation, resulting in premature motor failure.

The paper will discuss the specific mechanisms involved in the stator winding failure due to IFD's and present the measurements and analysis from surge monitoring installed on many different motors. Although some motors may experience short rise-time, high magnitudes surges, most motors experience either low magnitude and/or long rise-time surges, which are relatively harmless. Usually, several different magnitudes and rise-times are present from the same IFD. Thus, it seems that conventional motor stators can be safely used in many (but not all) IFD applications. Methods will be presented to determine when special IFD duty motors are needed. Voltage surge tests, as well as partial discharge tests, can help the user insure that motors can successfully operate in severe applications.

Introduction: Researchers have understood for over 70 years that fast rise-time voltage surges from a circuit breaker closing can lead to an electrical breakdown of the turn insulation in motor stator windings [1]. If the turn insulation is of an insufficient thickness, or has aged in service, the insulation will puncture when a short rise-time voltage surge occurs. Punctured turn insulation allows for a very high circulating current to flow into the affected copper turn, rapidly melting the copper conductors, which, in turn, results in a consequent burning/melting of the slot liner insulation, thus leading to a stator winding ground fault [2,3].

Rapid advances in power electronic components in the past decade have lead to a new source of voltage surges. Inverter-fed drives (IFDs) of the pulse width modulated (PWM) type that use insulated gate bipolar junction transistors (IGBTs) can create tens of thousands of fast rise-time voltage surges per second. Anecdotal evidence suggests that the huge number of voltage surges from IFDs can lead to gradual deterioration and eventual failure of the turn insulation - both in low voltage (less than 1000 V) and medium voltage (2.3 to 4.16 kV) motors [4-6]

This paper describes measurements of the surge voltage characteristics from a group of eight low voltage motors driven by IFDs. As described in this publication, two motors have repeatedly been subjected to unexpected stator winding failures. Inspection of the windings after failure indicated that the main cause of the failures is the voltage surge environment applied to the stator winding.

Review of the impact of voltage surges on LV stator winding insulation: An investigation of the surges applied to random wound stator windings by IFD's show that these surges may have frequency components up to 5 MHz or so. At such frequencies, the stator windings appear as a complex ladder network with low impedance capacitive shunts to ground. The capacitive shunts cause most of the applied surge voltage to be dropped across the first few turns in a stator winding.

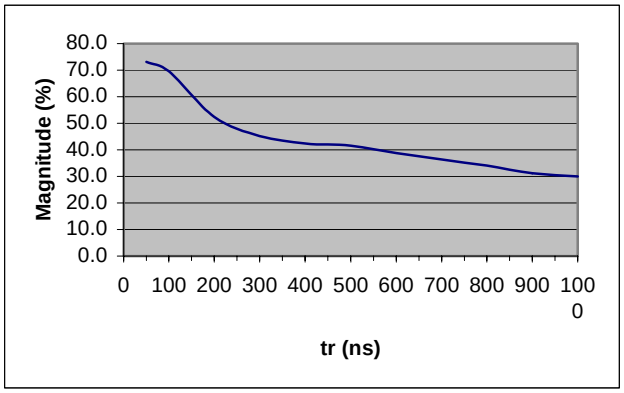

Figure 1: Voltage drop across first coil versus surge rise-time in a small random wound motor

By injecting a 5V pulse from a variable rise-time pulse generator (HP 8012) into a stator winding, and by measuring the voltage across the first turn with a differential very low capacitance probe, measurements were conducted to experimentally determine the amount of voltage that appears across the first turn in a stator winding, as a function of the voltage rise-time – see Figure 1. As much as 75% of the surge voltage applied to the terminals can be distributed throughout the first coil.

Furthermore, Figure 1 shows the voltage distributed across the first coil, relative to the surge magnitude, is inverse proportionate to the rise-time. The higher the voltage across the first turn, the higher the risk of experience a Partial Discharge (PD). Consequently, fast rise-time surges of higher magnitudes have a high risk of inducing PD in the random wound stator winding.

Figure 2 and Figure 3 show the surge waveform measured at the terminals of a 10 HP, 440 V squirrel cage induction motor fed by a 600 V pulse width modulated type of drive, which uses IGBT's. The waveforms were measured via an oscilloscope using low inductive resistive voltage dividers attached at the motor drive and the motor terminals. There is about 30 m of shielded triplexed power cable between the drive and the motor. This drive created 10,000 surges per second. The recorded waveforms had risetimes as short as 80 ns. The highest magnitude recorded was about 1200 volts, or about 3.3 per unit, with 1 pu corresponding to the rated peak line-to-ground voltage of the motor. In Figures 2 and 3 the top trace is the A phase signal at the drive. The other three traces are at the motor. The scope was in peak hold mode.

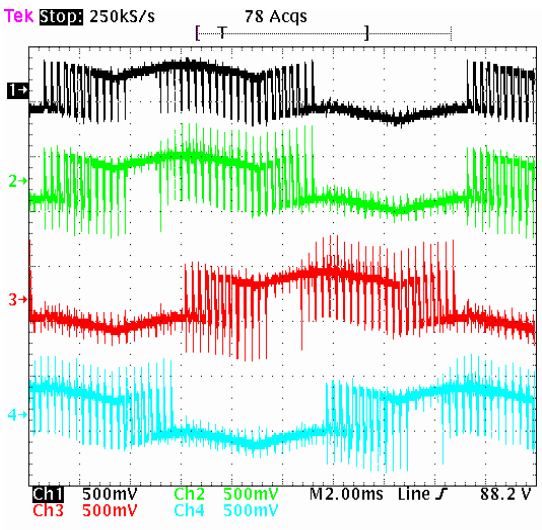

Figure 2: Surge Environment on a Motor. Ch. 1 is Aø at Drive, Ch. 2 is Aø at Motor, Ch. 3 is Bø at Motor, Ch. 4 is Cø at Motor, Vertical axis: 1: 2000.

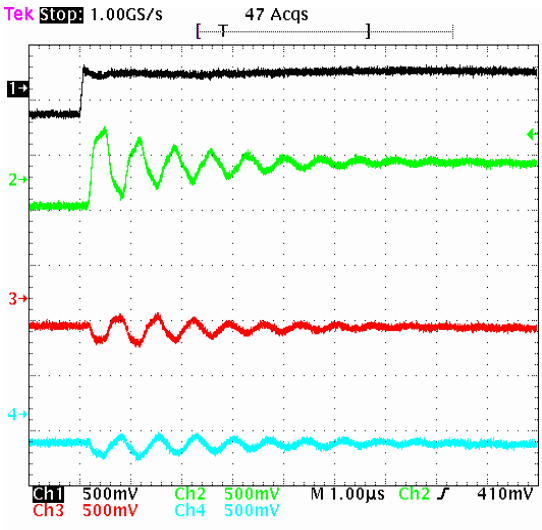

Figure 3: Zoom of an individual fast rise-time surge. Ch. 1 is Aø at Drive, Ch. 2 is Aø at Motor, Ch. 3 is Bø at Motor, Ch. 4 is Cø at Motor, Vertical axis: 1: 2000.

Figure 2, which shows a full AC cycle of applied voltage, shows that there is much more ring overshoot at the motor terminals resulting in bipolar surges of varying magnitudes. Thus, in order to characterize the surge environment, surge measurement must be carried out at the motor terminals and not at the drive.

Furthermore, Figure 3 shows one surge from the drive can create several surges at the motor terminals of different rise-times and magnitudes. Hence, the stator windings are subjected to a *distribution* of surges.

Thus, in conclusion, Figure 1 shows the shorter the rise-time, the greater the voltage across the first turn and the more dangerous becomes the surge to the motor. Therefore, by fully characterizing the surge environment applied to a random wound stator winding, one can assess the risk of stator failure due to electrical degradation.

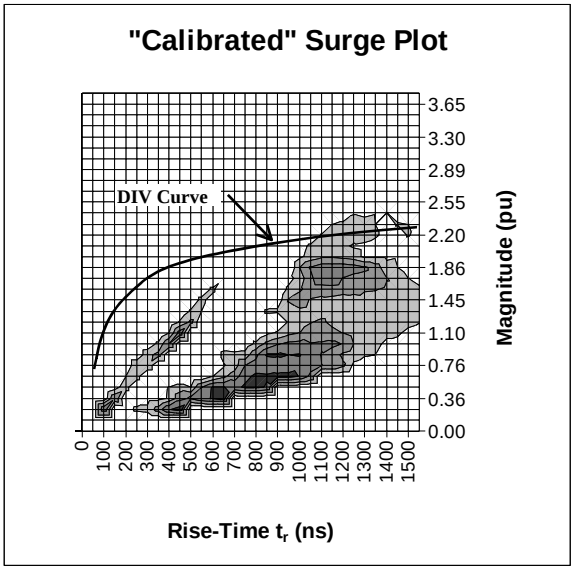

Figure 4: Example of a Calibrated Surge Plot [12].

Finally, as outlined in [12], the measured surge environment may be assessed quantitatively by performing Partial Discharge Inception Voltage (DIV) measurements as a function of rise-time for the stators examined. By superimposing the DIV curve on the measured surge plot, the surge plot is essentially calibrated with reference to which surges may give rise to partial discharges.

Surge Measurement System: As described earlier, IFDs create tens of thousands of voltage surges per second with varying magnitudes and rise times as fast as 50ns. As shown above, the voltage surges from an IFD pulse applied at the stator terminals may be measured by conventional means via a simple resistive voltage divider and a digital oscilloscope. This system allows for the measurement of the waveform of a given surge.

However, as discussed in [11], digital oscilloscopes exhibit an inherent limitation when used for recording surges: A vast majority of surges are ignored since a digital oscilloscope can only be triggered from 1 to 10 times per second, while 20,000 surges may occur in the same interval. Hence, only 1 in about 1000 surges can be recorded. In addition, the oscilloscope can normally only be triggered on the largest magnitude surges. As moderate magnitude surges, with very fast rise-times may be more damaging to the stator insulation than high magnitude/slow rise-time surges, it is likely that the oscilloscope may not trigger on the surges which, in time, are most likely to cause insulation failure.

In order to assess the severity of the electrical surge environment in which a motor operates, a reliable measurement of the distribution of electrical surges must be performed. The distribution of surges is defined by the magnitude, rise-time and repetition rate of each surge applied to the stator. When the exact surge environment is known, the surge distribution is said to be characterized. Thus, the surge environment cannot be characterized via conventional means.

To overcome the limitations outlined below, a special electronic instrument was developed. This device, SurgAlert™, measures the magnitude and rise-time of every surge that occurs within a given time interval. It also determines the total number of surges that a motor is subjected to during the measurement interval. However, this instrument cannot record the entire waveform of each surge. The monitor has the following specifications:

- Wideband (50 Hz to 10 MHz) resistive or capacitive voltage dividers, capable of operating on motors rated up to 13.8 kV. For motors rated 600 V or less, a resistive voltage divider is used. The dividers must be installed at the motor terminals.
- A portable electronic instrument, which is temporarily placed near the motor for the duration of the measurement, which digitally records the rise-time and magnitude of each surge, and stores this information in memory.
- A laptop computer that downloads a summary of the measured surges recorded in the measurement interval, for display or printout.

The data acquired may be exported to a computer file, which is readable by Microsoft Excel. It is thus possible to perform further processing of the data acquired. Reference 7 gives further details of the surge monitoring system.

In-service Failures Due to IFD's: Skaerbaek Power Station, Unit 3 is a combined power and district heating plant. The net electrical output is 390 MW. The plant was put into operation in July, 1997. A large number af variable speed drives have been installed for operation of pumps to reduce the unit´s house load. Motors rated 90 kW (120 H.P.) and below are mainly supplied from the 400 V busbar whereas motors rated above 90 kW (120 H.P.) are supplied from the 690 V bus bars. A total of nine motors, of which seven participate in this survey, are supplied from the 690 V bus bars. The size of these motors vary from 130 kW (175 H.P.) up to 1,890 kW (2,520 H.P.). All seven motors and the belonging inverters are from the same supplier. The basic data for the motors participating in this survey is given in Table 2

Since the commisioning two of the seven motors have been subjected to stator winding failures. One motor (850 kW) failed three times within the first 36 months of service and another motor (680 kW) failed once after 36 months. On the motor that failed three times, the third failure occured after less than 6 days of service. Operating hours and number of starts for the 2 motors that failed are given in Table 1.

After the first failure on Motor 1, the motor manufacturer was confronted with the suggestion that fast rise-time voltage surges originating from the IGBT inverter may have lead to the premature winding failure. This theory was rejected by the manufacturer who came to the conclusion that the failure was accidential and that it was quite unlikely that a similar failure would occur again.

Following the second failure on the same motor, the theory of fast rise-time voltage surges being the cause of failure was brought up again. Once more, this theory was rejected

Figure 5: Picture of Motor 1 After Failure

Motor	Application	Power Rating [kW]	Date of fault	Total operating hours	Number of starts
1	Main cooling pump	850	10-06-1998	2140	4
			10-02-2000	13044	119
			14-09-2000	13177	152
2	Condensation pump	680	13-10-2000	9440	753

Table 1: Failure Times for Motors 1 and 3

by the manufacturer. The conclusion was, as before, that the failure was accidental. The manufacturer accepted however to perform on site voltage measurements at the motor terminals in order to assure the customer that the failure was accidental and not caused by voltage surges. These measurements were performed only two days before the third failure on the same motor occurred.

One month later, a second motor failed. This failure lead to the decision to perform an independent measurement of the electrical surge environment on all 690 V motors, using the surge monitor.

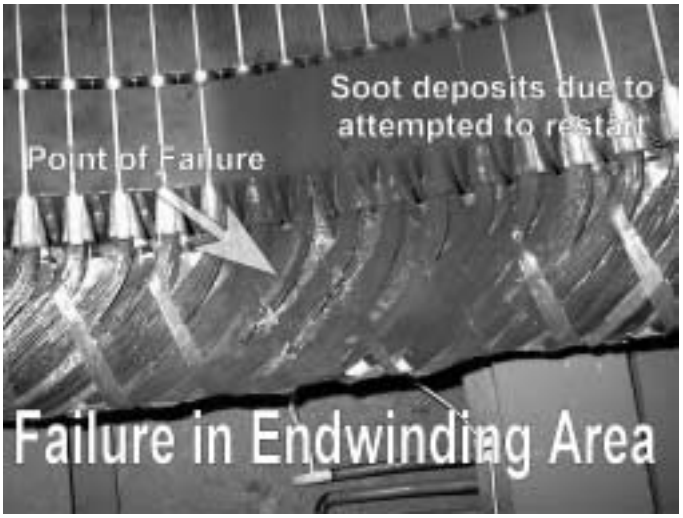

Figure 6: Close up of Motor 1 Failure

Although both motors that failed were still covered by the manufacturer guarantee, the unforeseen failures have lead to considerable expence to the power station.

Motor/IFD Configuration: The basic data for the motors participating in this survey is given in Table 2. The basic data for the motors participating in this survey is given in Table 2.
The following information on the specific winding design is given by the motor manufactor:

- The round wire is insulated with a quadruple build, class H enamel.

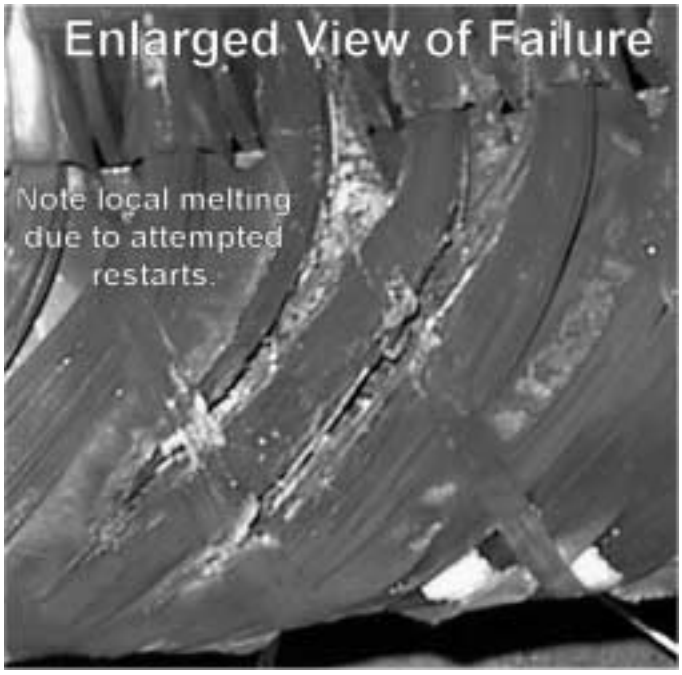

Figure 7: Enhanced Close Up of Motor 1 Failure. Local Melting of the Stator Winding Is Clearly Visible.

- The coils of different phases are completely seperated with mica paper on the overhangs.
- All the coils are separated with mica paper on the nose area.
- In the slots, the coils are insulated to ground and between each other with layers of NOMEX
- The winding is VPI impregnated in a special blend of class H, flexible and thixotropic resin.

The resin was oven cured and the stator turned while in the oven. Such a process gives an even coverage on the overhangs.

The motor manufactor insists that random wound motors with the above described specific design can be used for this type of application. Nevertheless motors supplied for similar applications at another Danish power station in 1999 were delivered with form-wound winding construction.

Motor	Application	Power Rating [kW]	Rated Voltage [V]	Drive Model	Cabel Type	Cable Length [m]
1	Main cooling pump	850	690	SVTL 1K2	XLPE	131
2	Condensation pump	680	690	SVTL 840	XLPE	114
3	Drain pump	130	690	SVTL 210	XLPE	75
4	Small pump	500	690	SVTL 600	XLPE	15
5	Main condensation pump	485	690	SVTL 600	XLPE	45
6	Main condensation pump	485	690	SVTL 600	XLPE	53
7	Big pump	1890	690	SVTL 2K4	XLPE	33

Table 2: Overview of tested motors.

Measurement Procedure: By attaching a clamp-on-type probe (a very low inductance resistive voltage divider) to the motor terminal of a given phase, a measurement of the surge environment of each phase could be performed. A three-dimensional surge plot characterizing the surge environment applied to that phase could thus be created.

Using alligator clips to connect to the motor terminals provides an easy and quick way to perform a measurement. The alternative is to temporally install low-inductive voltage dividers prior to performing the measurements. This ensures that the protection equipment will not trip the motor due to slight voltage imbalances between phases due to the increased load (from the instrument) on one phase. This option is more time consuming, as it requires down-time to install each voltage divider, and, in most cases, is not technically necessary. However, local plant regulations may, or may not, allow for connecting a probe during normal on-line operation.

First, two measurements were performed on the same phase of a motor: A 5 second measurement and a 10 second measurement. By normalizing the surge counts for each measurement into surge counts per second, a direct comparison between the two tests can be made.

This procedure allows for investigation of the consistency of the surge environment applied to the stator winding. If the surge environment is consistent, only one test is needed per phase to fully characterize the surges applied to the stator winding. This issue is discussed later in this publication.

The output is plotted as a three dimensional curve, see Figure 8, with the left scale being the magnitude of the voltage in p.u., the bottom scale is the rise-time of the surge in nanoseconds, and the vertical scale indicating the number of surges per second for each combination of surge magnitude and rise-time. Note that this is a log scale.

Often, a 2D representation of the three-dimensional plot is used – see Figure 9. A color scheme thus provides information of the surge count rate. As described earlier, the surges most likely to cause winding failure will have a short rise-time and high magnitude, that is, they will appear in the lower right part of the three-dimensional plot. A two dimensional representation allows for quick identification of these.

Results – The difference between phases: All phases were tested for all motors. The measurements showed that the surge environment measured on one phase was very similar to that measured on the remaining two phases. Figure 8 shows the surge plots for phases U, V and W of Motor 1.

As can readily be seen, there is no significant difference in the surge environment applied to each phase of the stator winding. This is hardly surprising as, from a theoretical point of view, the surge environment is defined by the output of the IFD drive.

The plots of Figure 8 are typical of those obtained on all eight motors tested, i.e. no significant differences in the surge environment could be detected between phases of a machine.

Furthermore, both 5 and 10 seconds tests were performed. Both tests were normalized to a 1 second test. A comparison between these tests showed similar surge distributions for the 5 seconds and 10 seconds test, which is indicative of consistent surge environment.

Hence, for interpretational purposes, only one measurement per phase is needed to address the severity of the surge environment applied to a given stator winding.

Results - Comparative Analysis: An initial inspection of Table 3 clearly shows motors 1 and 2 to be subjected to the highest surge environment in terms of pulse count rates and pulse magnitudes. The highest surge magnitude measured on Motor 1 was 3.5 per unit at a rise time of 1500ns whereas the highest surge magnitude measured on Motor 2 was 3.1 pu at a rise time of 1400 ns. Fortunately, these high surge magnitudes are measured at relatively high rise-times. Such high magnitude surges should not be too damaging to the insulation.

However, an investigation of the 2D plot for Motor 1 reveal the presence of a series of surges having rise-times of 100-650 ns with magnitudes ranging from 0.25 per unit to 2.2 per unit and repetition rates of 1-10 and 10-100 pulses per second – see Figure 9. The presence of these pulses is more of a concern than the presence of the maximum magnitude pulses of 3.5 p.u. at a rise time of 1200ns having a repetition rate of 1 per second. As

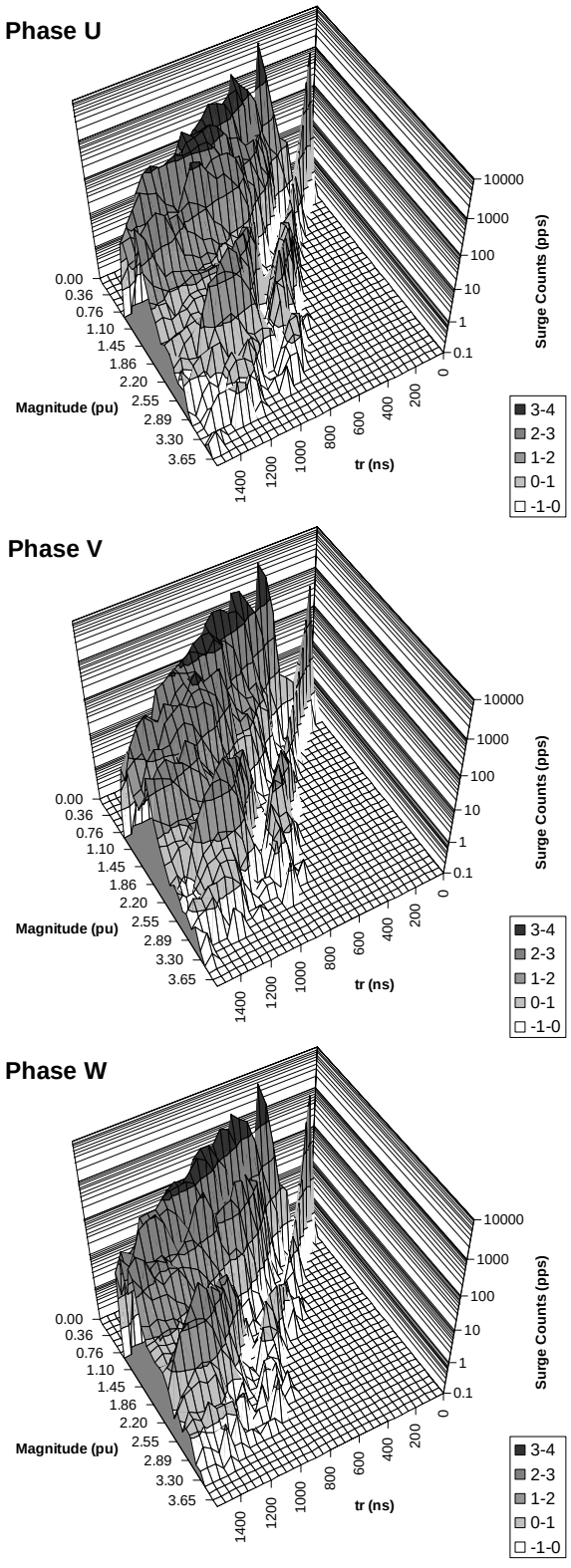

Figure 8: Surge Environment for Motor 1

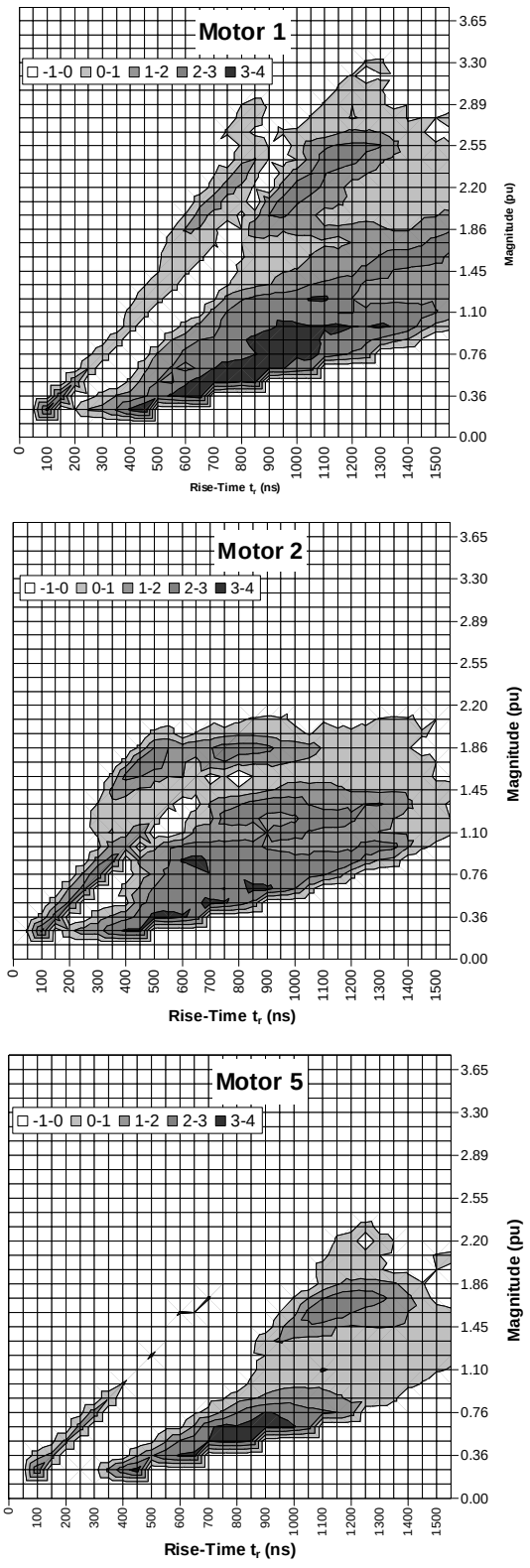

Figure 9: 2D Surge Plot for Motors 1, 2 and 5

Motor	Max. Magnitude [pu, ns]	Fastest Risetime [pu, ns]	Max Slew Rate [pu/µs]
1	3.51, 1500	0.24, 50	5.1
2	2.34, 900	0.24, 50	6.0
3	3.09, 1400	0.24, 50	5.3
4	2.20, 900	0.24, 50	5.3
5	2.41, 1100	0.24, 50	3.8
6	2.41, 1100	0.24, 50	4.0
7	1.44, 950	0.24, 50	3.7
8	2.41, 700	0.24, 50	5.8

Table 3: Result Summary of Tests

mentioned earlier, the higher the rise time, the higher the electrical stress between turns or phases. Hence, although not being of alarmingly high magnitudes, the faster rise time pulses measured on Motor 1 may be of a concern with respect to aging of the stator insulation.

Furthermore, the 2D plot indicates two types of surges: Initial surges created by the IFD and secondary surges possibly created by resonance phenomena. This is indicated by the general separation of surges into two “islands” in the plot – see Figure 9. The surge environment measured on Motor 1 constitutes the most significant surge environment measured so far using the SurgAlert technology. The data showed that similar observations can be made for Motor 3.

Table 3 show the highest slew rate measured for Motor 1 is 5.1 and 5.3 for Motor 2. These slew rates can be classified as being moderately high compared to the highest slew rate of 8.1 per unit measured so far on other machines elsewhere.

The surge environment for Motor 2 is also given in Figure 9 and can be characterized by a maximum pulse magnitude of 2.34 per unit at a rise time of 900 ns. The measured slew rate is 6 and that constitutes the highest slew rate measured on these motors. As such, it can be argued from a general point of view, that this motor is subjected to the “worst” surge environment of all the motors measured in this test. An investigation of the surge plot shows the initial surges for Motor 2 to have noticeable higher repetition rates than those measured for Motors 1 and 3.

The surge environments measured for the

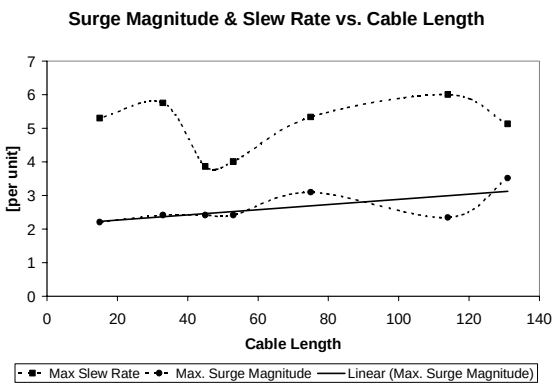

Figure 10: Surge Magnitude and Slew Rate As a Function of Cable Length.

remaining five motors are, without doubt, of less concern. As can be seen from Table 3, the maximum surge magnitudes measured are noticeably lower than those measured on Motors 1, 2 and 3. This is consequently expressed in the 2D surge plots – an example from Motor 5 is given in Figure 9. The slew rates, however, appear to be moderately high for the remaining 5 motors with Motor 6 yielding a slew rate of 4. This is the lowest slew rate detected for the eight motors measured in this test.

Common for all motors, the lowest rise time measured was 50 ns yielding surges having a magnitude of 0.24 per unit. Although this rise time can be categorized as short, it should be noted that the measured magnitude is relatively low.

Results – The influence of cable length: Figure 10 shows the relationship between calculated maximum slew rate and cable length for each measurement. It furthermore shows the relationship between maximum measured surge magnitude as a function of cable length. Figure 10 suggests that a clear relationship between maximum surge magnitude and cable length exists: The surge magnitude appear to increase with increasing cable length. Given the nature of travelling wave theory, this is not a surprising result.

In the case of the maximum slew-rate, Figure 10 suggests that the maximum slew-rate does not directly depend on the length of the cable connecting the motor to the IDF drive. The slew rates is defined as the ratio between the surge magnitude and surge rise time. As documented in Table 3, the rise-times measured for the maximum surge magnitudes range from 700 ns to 1500 ns thus giving rise to an erratic distribution of slew-rates for increasing surge magnitudes. Figure 10 thus suggest that the slew-rate is a secondary effect of the cable length and it can thus not be concluded that the longer the cable length, the more damaging the surge environment is.

Partial Discharge Inception Voltage: The basic principle of the test setup is sketched in Figure 11. Via a Baker Surge Tester, Model D12000, a 50 ns rise-time surge voltage is applied to an insulation sample or a stator winding. If of sufficient magnitude, the surge voltage will give rise to a partial discharge. The partial discharge give rise to a high frequency current signal, which is consequently extracted from the surge via specialized instrumentation, PDAlert™, connected in series between the surge source and the insulation sample. The net output from the instrument is a voltage signal originating from the partial discharge current pulse itself. An example from Motor 1 is given in Figure 12. The leads connecting the various components of the test setup are kept as short as possible.

The test procedure is described thoroughly in [12] but repeated in short here: Having connected a stator to the surge source, the surge magnitude was increased with approximately 200 volts per second from zero volts until a partial discharge was observed. The surge magnitude was then quickly decreased to zero volts. The

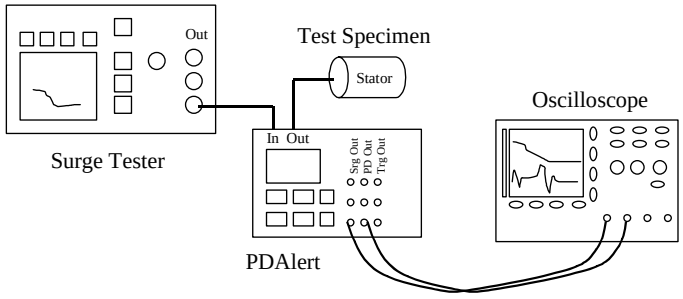

Figure 11: Sketch of DIV Test Setup

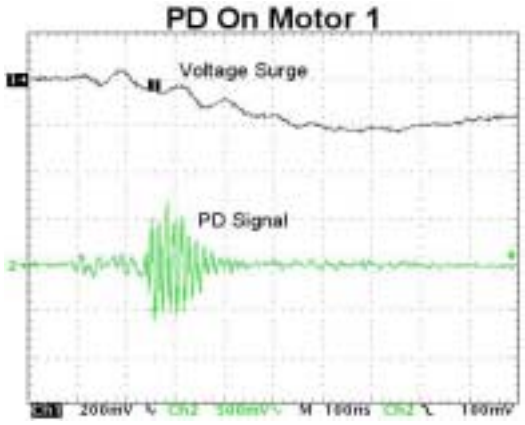

Figure 12: Example of PD on Motor 1

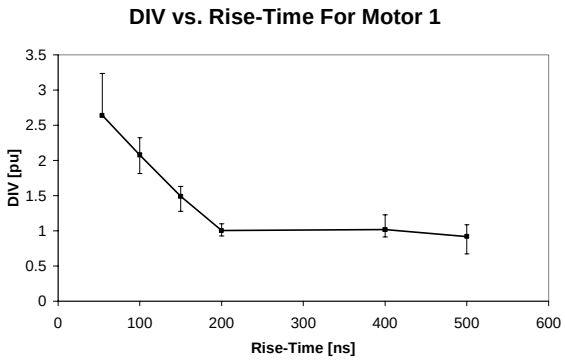

Figure 13: Discharge Inception Voltage vs. Rise-Time For Motor 1.

procedure was repeated seven times for each rise-time. Based on this, the mean (average) DIV was calculated for each rise-time. In addition, the ambient temperature and humidity was logged.

The average discharge inception voltage was 1.73 per unit for Motor 3. For Motor 1, the average DIV was 2.38 per unit. Table 3 shows that the maximum magnitudes - of surges having rise times up to 1550ns – is below the DIV for these motors. That strongly indicates that these motors are subjected to partial discharges, during normal operating conditions, due to the surge environment applied to the stator windings from the IFD and the connection cables.

A curve of the DIV versus rise-time for Motor 1 is given in Figure 13. The curve shows the DIV to decrease with decreasing rise-time. This is surprising as other curves obtained on new stators prior to being put into service shows the opposite relationship, namely an increase in DIV with increasing rise-time as explained by the distribution of voltage across the first turn as a function of surge rise time.

Figure 14 shows the measured surge plot for Motor 1 with the DIV curve super imposed. Surges above the curve may give rise to PD whereas surges below the curve will not give rise to PD.

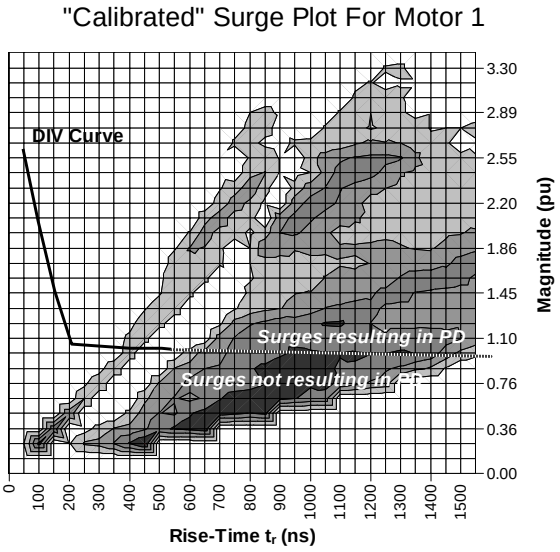

Figure 14: Calibrated Surge Plot for Motor 1

As can be seen from [12], the DIV measured on these motors are low compared to those measured on virgin stators. The results obtained on virgin stators showed DIV's of between 6 per unit to 9.5 per unit – as seen from Figure 15 where Stators 1 and 2 are virgin stators and Stator 3 constitutes the DIV for Motor 1 [12].

Compared to the results obtained on virgin windings and presented in [12], these results indicate that for aged windings, i.e. windings subjected to real operating conditions, DIV is more related to the surge magnitude rather than the rise-time coupled with the probability for occurrence of a free electron, which increases with increasing (slowing) rise-time.

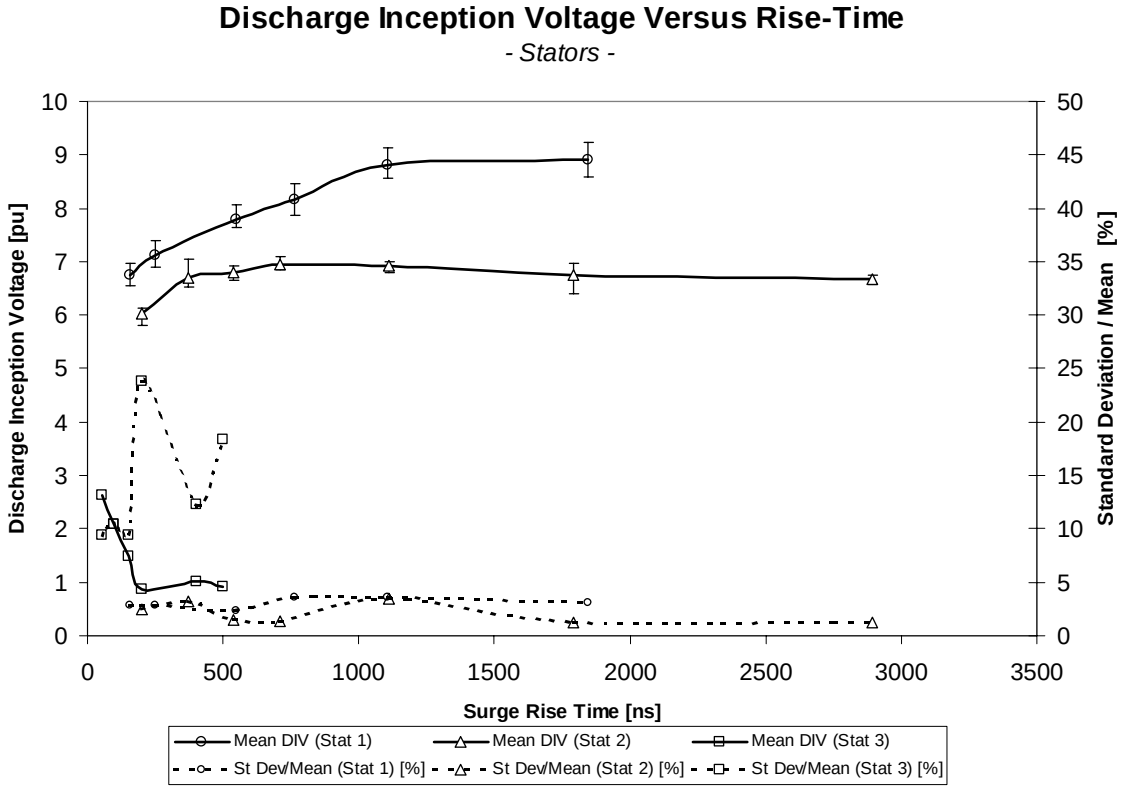

Figure 15: DIV's for Motors of Different Design And Size [12]

Discussion: The measurements clearly showed Motors 1 and 2 to be subjected to a surge environment which must be perceived as having a negative impact on the stator winding insulation and its estimated life time.

Confronted with the measurements performed using the SurgAlert instrument, the motor manufactor have accepted to supply and install filters on 5 of the 9 motors. Filters have already been installed on the 850 kW motor that failed 3 times and will be installed on the remaining four motors as soon as possible.

Filters are simple 20 μH reactors connected in series with the motor at the cable outlet from the inverter. The impact of these reactors are not known at present. Preventive filters have been installed on Motors 1 and 3. Additional surge measurements are to be be performed once installed. The measurements will thus clearly document the effect of filters.

The Discharge Inception Voltage measurements strongly indicated that the surge environment applied to Motors 1 and 3 gave rise to partial discharge activity.

Conclusions: The surge measurements clearly showed the two motors previously to have experienced failures to be subjected to the worst surge environments of the motors measured here. Furthermore, the DIV measurements performed on Motors 1 and 2 clearly documented that the Discharge Inception Voltages, under surge conditions, were lower than the max surge magnitudes measured on-line during normal on-line operations. This strongly indicate that the root cause of the failures experienced were indeed the presence of partial discharges.

Also, the measurements showed little difference in the applied surge environment between phases on the individual machines indicating when performing this types of measurements, measuring one phase per motor should be sufficient.

Furthermore, when purchasing inverter drives intended for 690 V supply, the manufacturer should be asked to indicate acceptable surge levels at the motor terminals, and should be required to preform measurements of the actual surge inviroment when the motors are being commisioned.

Acknowledgements: The authors would like to thank Jens Aage Jensen of SV Production for his cooperation on the work presented in this publication.

References:

[1] E.W. Boehne, Voltage Oscillations in Armature Windings Under Lightning Impulses, Trans AIEE, 1930, p1587.

[2] M.T. Wright, S.J. Yang, and K. McCleay, General Theory of Fast-Fronted Interturn Voltage Distribution in Electrical Machine Windings, Proc. IEE, Part B, July 1983, p 245.

[3] B.K. Gupta, et al, *Turn Insulation Capability of Large AC Motors,* Parts 1, 2, 3, IEEE Trans EC, December 1987, p 658.

[4] A.L. Lynn, W.A. Gottung, D.R. Johnston, *Corona Resistant Turn Insulation in AC Rotating Machines,* Proc. IEEE Electrical Insulation Conference, Chicago, October 1985, p 308.

[5] W. Yin, et al, *Improved Magnet Wire for Inverter-Fed Motors,* Proc. IEEE Electrical Insulation Conference, Chicago, September 1997, p. 379.

[6] E. Persson, *Transient Effects in Applications of PWM Inverters to Induction Motors*, IEEE Trans IAS, September 1992, p1095.

[7] G.C. Stone, S.R. Campbell, M.Susnik, *New Tools to Determine the Vulnerability of Stator Windings to Voltage Surges form IFDs*, Proc. IEEE Electrical Insulation Conference, Cincinnati, October 1999, p 149.

[8] L. Saunders et al, *Riding the Reflected Wave*, Proc. IEEE Petroleum and Chemical Industry Conference, September 1996.

[9] E.P. Dick et al, *Practical Calculation of Switching Surges At Motor Terminals*, IEEE Transactions On Energy Conversion, December 1988, Vol. 3, No. 4, p 864.

[10] C. Lanier, A Novel Technique For The Determination of Relative Corona Activity Within Inverter-Duty Motor Insulation Systems Using Steep-Fronted Voltage Pulses, IEEE Conference Record of The International Symposium on Electrical Insulation, Arlington, VA, June 1998, p 229.

[11] G.C. Stone, S.R. Campbell and S. Tetreault, *Inverter Fed Drives: Which Motor Stators are at Risk?,* IEEE Industrial Applications Magazine, p. 17 f.f. September 2000.

[12] M. Fenger, S. R. Campbell and G. Gao, “The Impact of Surge Voltage Rise Time on PD Inception Voltage in Random Wound Motors of Different Designs”, 2001 Annual Report - Conference on Electrical Insulation and Dielectrics Phenomena, pp. 352-355, October 2001.